On the Response of Leading-Edge Phenomena and Near-Wake Formations to Trailing-Edge Flap Actuation

Albert Medina* and Matthew Rockwood
Air Force Research Laboratory, Wright-Patterson AFB, OH 45433

ABSTRACT

In this work, the response of a separated flow field and free shear layer of a NACA 0006 wing to rapid mechanical actuation of a conventional trailing-edge flap is studied in a nominally two-dimensional flow at a chord-based Reynolds number of 4×10^4. We report on the transient lift response to rapid step-and-hold maneuvers and the response of the near-body wake to sustained harmonic pitching of the flap. The term "rapid" is reserved here for motions performed within one convective time. The wing is fixed at $\alpha = 10^\circ$ and 20° for representative separated and massively-separated flow fields, respectively. In both kinematic cases the amplitude of flap motion is low, measuring 1°. It is shown that the rapid motion of the trailing-edge flap is sufficient to induce flow reattachment or rollup of the separated shear layer into a leading-edge vortex. Under harmonic flap excitation, it is shown that authority of near-body wake shedding characteristics may be imposed even for the separated transitional case of $\alpha = 10^\circ$.

1 INTRODUCTION

The mitigation, control, and exploitation of separated flows ranks with turbulence as one of the great unresolved problems in aerodynamics. Principal applications pertain to small flight articles where skin friction drag is not the primary driver of aerodynamic performance. Such small flight articles are renowned for their agility and maneuverability, often allowing the article to perform large excursions momentarily from steady cruise flight conditions. Due to the scale, however, small flight articles may be rendered particularly susceptible to relatively large disturbances in the flow field. In both instances, be it the article's high maneuverability or incurred flow disturbances, the article is subjected to temporal variations in aerodynamic loading accompanied by transient vortical phenomena. If left unabated, the asymptotic state of transient flows is outright separation of the lifting surface. In such instances of extensive separation, the question arises as to whether it is preferable to reduce separation to attain the putatively higher aerodynamic efficiency, or whether it is preferable to manage the separated flow to produce a favorable aerodynamic effect, such as higher lift. To this end, the proper characterization of the dynamic response of the flow to actuator input is imperative for the development of effective active flow control solutions. In this study we propose the use of mechanical actuation of the trailing-edge flap to induce a transient response in aerodynamic loading from rapid flap-step input and explore the effects on near-body shedding dynamics from sustained harmonic flap motion.

Conventional active flow control techniques have proven an established ability to force flow reattachment over separated surfaces when actuation is applied continuously, the reattachment effects persist for the duration of actuation [1, 2]. When applied in short burst or as discrete singular input events, the impulse-like disturbance introduced by the flow control technique excites a broad spectrum of the separated flow which triggers multiple instabilities for an effect that persists substantially longer than the duration of actuation. However, a key feature shared among these impulse-like techniques is a transient lift response that bears a lift-reversal spike at the onset of actuation. Such a spike presents a challenge from the perspective of real-time flow control: this presents an inherent delay in the system, limiting the bandwidth of control [3].

The performance of a lifting body, certainly within an unsteady regime, is significantly altered by the dynamics of the near-body wake [4] be it induced by body motion, excited by application of flow control actuators, or naturally occurring feature of the flow. For a given static airfoil there exists a critical Reynolds number by which a Hopf bifurcation[5] occurs. The result is an oscillatory wake, in contrast to the steady, separated flow field of the sub-critical regime. At sufficiently high Reynolds number in the super-critical regime the oscillatory wake transitions to vortex shedding. When a given airfoil is driven in harmonic motion, synchronization between the rigid body's dynamics and the vortex shedding frequency may be exploited to yield departures from standard performance. Indeed, such resonant behavior was exploited by Choi *et al.* [6] in surge and plunge motions where time-averaged forces were significantly changed when the airfoil was driven at the vortex shedding frequency and its subharmonic. To similar effect, Dawson *et al.* [7] demonstrated substantial increases in aerodynamic loading in resonant pitching. Further, it was shown that substantial lift may be yielded for airfoil pitching at specific frequencies when the airfoil is separated but wake is steady. That is, there exist con-

*Email address: alberto.medina.3@us.af.mil

figurations in which vortex shedding being induced by airfoil motion can enhanced loading akin to resonant behavior. Such behavior was explore by Cleaver *et al.* [8] as a high-lift mechanism where low-amplitude plunge oscillations of an airfoil at zero angle of attack experienced stable deflected jets of vorticies responsible for large lift coefficients. The frequency of natural vortex shedding at elevated Reynolds numbers and angles of attack appears to satisfy a Strouhal range of $St = 0.13 - 0.20$, as demonstrated by Huang and Lin [9]. At such Reynolds numbers moderate attack angles are transitional and the wake does not reflect the Strouhal number criteria.

In this study, the response of a separated flow of a NACA 0006 wing to rapid-actuation of a conventional flap are explored. The airfoil is bisected about the midchord to a test article comprised of 50% leading edge and 50% trailing-edge flap. The leading-edge element is held fixed (α_{LE}) while the flap is allowed to pivot about the airfoil midchord (δ). The receptivity of varying degrees of separation to rapid step-and-hold maneuvers by the flap is examined by comparison of two representative flow states: $\alpha = 10^\circ$ corresponding to a separated flow, and $\alpha = 20^\circ$ corresponding to a massively-separated flow. In these comparisons, the flap executes a rapid step of $\pm 1^\circ$ from an initial planar configures ($\alpha = \delta$). "Rapid" motions are performed within a fraction of a single convective time. We elect to employ mechanical actuation to avoid delay or "dead time" associated with conventional fluidic actuators, but instead seek to attain an instantaneous aerodynamic response to flap actuation, rooted in bound circulation following Wagner's solution to impulsive change in flap deflection [10]. Lastly, the effects of sustained low-amplitude harmonic flapping on the near-body wake shedding dynamics is explored for the separated case of $\alpha = 10^\circ$ where we seek to impose authority over the shedding frequency for a flow regime that is historically transitional.

2 Experimental Setup

Experiments were performed in the Air Force Research Laboratory (AFRL) Horizontal Free-Surface Water Tunnel (HFWT). The tunnel is outfitted with a three-degree-of-freedom motion stage, consisting of a suite of linear motors, allowing the test article to engage in pitch, plunge, and surge maneuvers (or combination thereof). The test article is a NACA 0006 airfoil measuring 200mm in chord that spans the width of the water-tunnel test section (457.2mm) to produce a nominally two-dimensional flow field. The airfoil is bisected about the midchord, as shown in Fig. 1, to construct a trailing-edge flap of 50% chord. The resulting fore element is held fixed at a static incidence angle (α_{LE}) while the flap is pivoted about the midchord to execute a specified kinematic schedule.

Direct force measurements were acquired via two six-component force/moment balances. Both the fore element and the flap element were supplied a dedicated force balance. This arrangement allowed for the independent measurement of the constitutive elements' aerodynamic loading history. The fore element and the flap do not communicate mechanically, but instead are hydrodynamically coupled with a midchord gap of 0.5 mm separating the two. Planar flow visualization was conducted by the illumination of a fluorescent dye. Illumination was provided by laser sheet optics positioned at the three-quarter span position, and dye was introduced into the flow field through dye ports located at the leading and trailing edges of wing. Further detail can be found in Ref. [11, 12, 13].

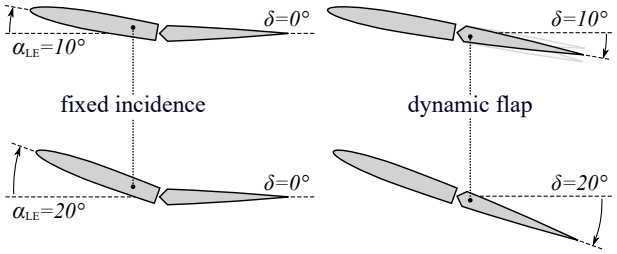

Figure 1: NACA 0006 test article configuration: (*top row*) $\alpha_{\mathrm{LE}} = 10^\circ$, (*bottom row*) $\alpha_{\mathrm{LE}} = 20^\circ$.

This study examines the response of separated flow to a excitation input in the form of rapid trailing-edge flap deflection at a chord-based Reynolds number of $Re = 4 \times 10^4$. Conveniently, the freestream speed and chord length provide for a convective time that equates to 1.0 s of wall-clock time. The distinction of "rapid" is reserved here for maneuvers by the flap that are completed in a fraction of one convective time. This study concerns discrete excitation of a singular step-and-hold maneuver by the flap as well as the effects of sustained actuation of the flap in harmonic deflection. For harmonic deflection the flap is driven in a sinusoidal schedule with a deflection amplitude of 1° (for $\alpha = 10^\circ$: $\delta = 11 \rightarrow 9^\circ$, for $\alpha = 20^\circ$: $\delta = 21 \rightarrow 19^\circ$) and frequency 6Hz ($TU/c = 0.167$). The step-and-hold maneuvers follows from a C^∞-smoothing ramp function formulated by Eldredge *et al.* [14]. Here, however, the smooth ramp has been fitted to a semi-period of a sinusoidal waveform, providing a step in deflection angle of $\pm 1^\circ$. For $\alpha = 10^\circ$ this entails a flap motion of either $\delta = 10 \rightarrow 11^\circ$ or $10 \rightarrow 9^\circ$. And for $\alpha = 20^\circ$ this entails a flap motion of either $\delta = 20 \rightarrow 21^\circ$ or $20 \rightarrow 19^\circ$. The step in deflection angle by the smooth ramp, although small in amplitude, appears rather steep and is interpreted akin to an impulse in bound circulation. Because the geometry of the airfoil is tied directly to the mode of excitation, the deflection amplitude is selected such that deflection does not result in a geometry that deviates greatly from the baseline undeflected airfoil flow.

3 RESULTS

3.1 Baseline Flow

We begin with examination of the baseline flow field states of interest, as depicted in Fig. 2. Two flow states are considered in assessing the potential control authority of the flap engaged in rapid maneuvers. These states correspond to $\alpha_{\mathrm{LE}} = 10^\circ$ and $\alpha_{\mathrm{LE}} = 20^\circ$ and represent prototypical separated and massively separated flow fields, respectively. In the instances of Fig. 2 the wing is held static in a freestream and the flap deflection angle (as measured with respect to the horizontal plane) is equal to the leading-element incidence angle ($\delta = \alpha_{\mathrm{LE}}$) to provide a planar airfoil. Both orientations $\alpha_{\mathrm{LE}} = 10^\circ$ and 20° are distinguished by their separated shear layer emanating form the wing leading edge, where the case of $\alpha = 20^\circ$ exudes further expulsion of the shear layer and expansion of the separation envelope. As anticipated, the time-averaged lift-to-drag ratio incurs a decrease with increasing severity of flow separation. At $\alpha_{\mathrm{LE}} = 10^\circ$ aerodynamic performance measures $\overline{L/D} = 3.662$ and measures a reduced value of $\overline{L/D} = 2.547$ for 20°.

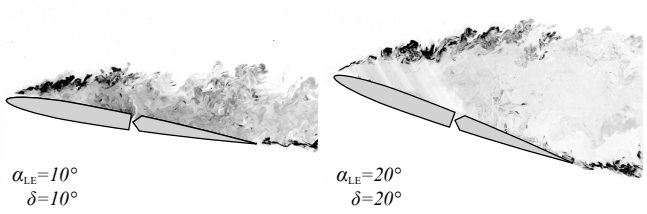

Figure 2: Baseline flow fields of static airfoils: (*left*) $\alpha_{\mathrm{LE}} = 10^\circ$ separated flow, (*right*) $\alpha_{\mathrm{LE}} = 20^\circ$ massively separated flow.

3.2 Transient Flap-Step Response

The effect of a rapid step in deflection angle by the trailing-edge flap is studied here through direct force measurement. As previously noted, the flap performs a step in deflection angle amounting to a pitch-and-hold maneuver. Because this maneuver is interpreted here as a surrogate for a bound-circulation impulse, the direction of flap pitch should induce directional-dependent responses as the circulation sign correlates with pitch direction. Thus, a small amplitude step is supplied of $\Delta\delta = \pm 1^\circ$ from the initial planar configuration of $\alpha_{\mathrm{LE}} = \delta$.

Beginning with the separated case of $\alpha = 10^\circ$, Fig. 3 shows the time history of lift in response to a flap rapid step. Lift is displayed as a differential value measuring the temporal deviation in lift from the initial static mean value. Mean values for all initial and final geometric configurations considered in this study are summarized in Table 1 for convenience. Prior to motion both the $+1^\circ$ and -1° lift curves track well with the time-averaged static lift value, indicated by the grey horizontal line. Upon executing the deflection step at $t^* = 5$ (where $t^* = tU/c$) there exists a rather sharp, yet brief, inertial spike. Directly thereafter the lift curve demonstrates an immediate response with a resulting lift value differing from the initial static value. The transient lift profile initiates with an effective vertical shift in value from the pre-deflection state. This immediate response is in contrast to the performance of some conventional fluidic actuators which when pulsed suffer from lag or deadband prior to realizing the desired response.

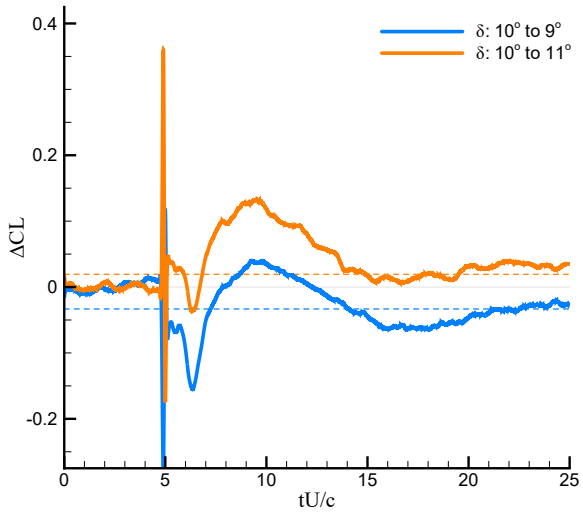

Figure 3: Transient response for $\alpha_{\mathrm{LE}} = 10^\circ$: (*grey line*) $\overline{\mathrm{CL}}|_{\delta=10^\circ} = 0.6943$. (*dash line*) Time-averaged static lift of final step angle.

α_{LE}	δ	$\overline{CL}$	$\overline{CL1}$	$\overline{CL2}$
10°	10°	0.6943	1.1629	0.2258
	9°	0.6619	1.1343	0.1859
	11°	0.7127	1.1601	0.2625
20°	20°	0.7954	1.1538	0.4399
	19°	0.7624	1.1148	0.4109
	21°	0.8556	1.2236	0.4852

Table 1: Time-averaged static lift values.

As previously discussed, the current mechanical mode of excitation is coupled with the geometry of the airfoil. Thus the long-time behavior of the lift curve in "hold" is best characterized as a relaxation to a new steady asymptotic value denoted in Fig. 3 as the dashed lines. In a $\Delta\delta = +1^\circ$ maneuver, the terminal geometry provides for a net positive camber. Conversely, for -1° there results a net negative camber. As such, the relaxation values of lift differ from the undeflected airfoil, with $\Delta\delta = +1^\circ$ exceeding initial lift production ($\delta = 10^\circ$) and -1° generating a reduction in steady lift.

Despite differences in asymptotic relaxation lift values,

the two modes of flap deflection exhibit significant transient responses with temporal histories bearing a remarkable resemblance. The transient lift profile trends among the two deflection cases initiate with a nominal plateau value which persists for approximately one convective time followed by a steep dip. Recovery from the dip is sharp, with the entire recovery event occurring over approximately one convective time. The lift profile continues to climb over the next three convective times to achieve a global transient peak, followed by a gradual relaxation over the next several convective times. Post inertial-spike, the relative magnitudinal differences from peak-to-peak lift appears preserved among the two cases. However, the two cases are distinguished by their initial vertical shift in lift. For the positive-camber motion, the transient lift profile is elevated to instantaneously exceed even the final static lift value of $\delta = 11°$. This is in contrast to the negative-camber motion where the transient profile appears to experience a downward shift from the pre-motion value, falling below even the static lift value of $\delta = 9°$.

As previously mentioned, the test article is equipped with a dedicated load cell per wing element. This configuration allows for inspection of the respective contributions to lift between the leading-edge element and the flap. This is particularly utile when only a subset of components of the wing's articulated body are driven in motion while the remaining components are held fixed in space. The fixed leading element's response comes as an artifact of its proximity to the driven flap through hydrodynamic coupling. The resulting transient lift histories are shown in Fig. 4 where CL1 refers to the leading element and CL2 the flap element. Lift coefficients here are normalized by their respective chordwise segment lengths (for this geometry $\hat{c} = c/2$). As previously observed, the transient profiles of both cases appear quite similar, with the resulting changes in lift differing nominally by way of vertical offset from the pre-motion value of lift. The flap suffers from a momentary anti-lift spike prompting a negative lift differential, ΔCL2, independent of the deflection direction. However, the vertical lift offsets (post inertial spike) remain directional-dependent. The apparent drop in CL (Fig. 3) for $\Delta\delta = -1°$ appears predominantly incurred by the fixed leading element where the apparent vertical offset in lift is most severe.

Thus far the influence of flap step-direction has been limited to the vertical offset in lift, bearing negligible command of the transient profile or response time for a separated flow corresponding to $\alpha = 10°$. Only when the flow field is progressed to a massively separated state does the step direction offer divergence in transient profile characteristics for the seminal cases of $\Delta\delta = \pm 1°$. To achieve the desired separation the airfoil is realigned with the leading element fixed at $\alpha_{\mathrm{LE}} = \delta = 20°$ (Fig. 2). The lift response for the representative massively separated flow is show in Fig. 5. As before, prior to motion ($t^* < 5$) the phase-averaged lift tracks well with the time-averaged static lift value ($\overline{CL} = 0.795$). Barring the inertial spike at $t^* = 5$, the transient response to a flap step of $\Delta\delta = +1°$ is marked by the instantaneous realization of the long-time static lift value. It is without cunctation or developmental rise that the lift for a positive-camber step achieve the asymptotic value of the newly configured airfoil ($\delta = 21°$). This stands in contrast to conventional fluidic actuators which when employed in discrete pulsing induce an initial anti-lift spike upon actuation. Approximately one convective time after the motion is completed, the case of $+1°$ experiences successive peaks of diminishing magnitude with the initial lift peak occurring near $t^* = 7.5$.

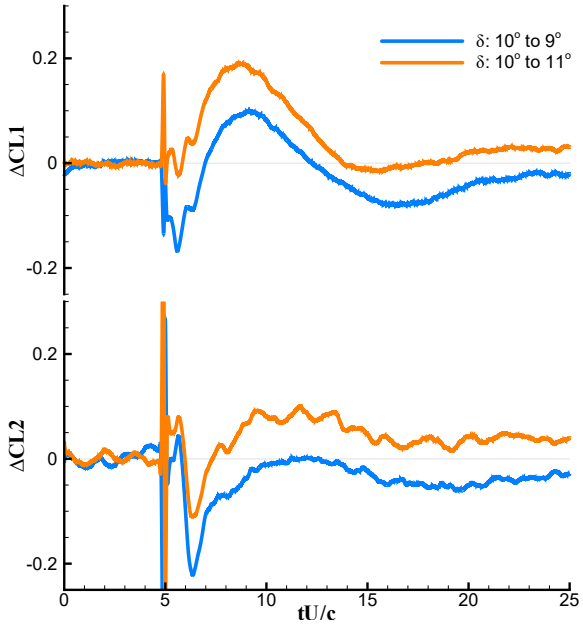

Figure 4: Transient response for $\alpha_{\mathrm{LE}} = 10°$: (*top*) leading element CL1, (*bottom*) flap element CL2.

When the flap is driven in step toward a negative camber ($\Delta\delta = -1°$) the response garnered in lift is drastically altered from the positive-camber counterpart. The vertical negative shift in lift remains a prominent feature just as before in $\alpha = 10°$. The negative shift lies well below the static value of both $\delta = 20°$ and $19°$. However, approximately one convective time thereafter, the transient lift signature undergoes a substantial transformation in its aggressive upward surge. The steep rise in lift readily exceeds the initial undeflected static state ($\delta = 20°$), culminating in a global peak approaching $t^* = 7.5$. Note that the peak lift induced by the negative-camber step nearly doubles that of the positive-camber motion. During relaxation there exists a minor peak nearly coincident with the secondary peak cited for the positive-camber step approaching $t^* = 10$. In both step-direction cases the relaxation time remains intact. Relaxation is nominally achieved approximately 10 convective times after the deflection step is executed. This scaling is consistent

with the separated case ($\alpha = 10°$) suggesting the transient dynamics scale with convective time.

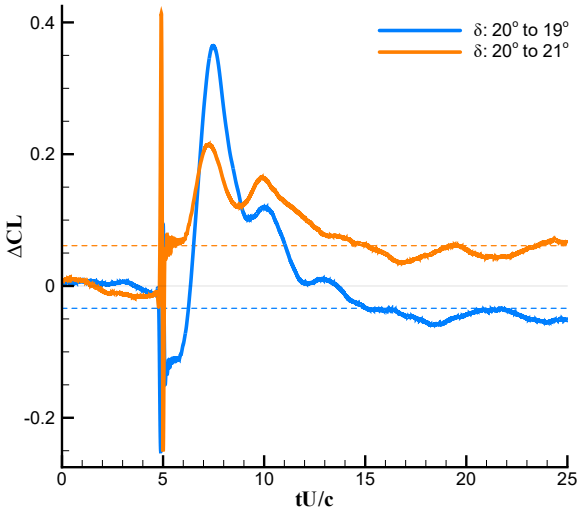

Figure 5: Transient response for $\alpha_{\mathrm{LE}} = 20°$: (*grey line*) $\mathrm{CL}|_{\delta=20°} = 0.7954$. (*dash line*) time-averaged static lift of final step angle.

The respective contributions to lift from both the leading- (ΔCL1) and flap element (ΔCL2) are displayed in Fig. 6. Inspection of the lift histories associated with $\Delta\delta = +1°$ and $-1°$ reveal striking commonalities between the two cases. Indeed, many of the overall trends among the two cases' profiles in Fig. 5 and Fig. 6 appear common, though with differing temporal scaling. It is understood that there exists some interaction between the flap and the separated shear layer for both the separated and massively separated flows. The mechanisms by which the step modes affect the flow fields governing the resulting transients is provided some clarity through flow visualization in the following section.

3.3 Flow Visualization of the Flap-Step Response

Investigation of the massively separated flow ($\alpha = 20°$) response to a negative-camber step ($\Delta\delta = -1°$) in Fig. 7 reveals large scale rollup of the leading-edge shear layer, as found in [12]. By $\Delta t^* = 0.56$ (where Δt^* is the duration of time elapsed since the completion of motion) the leading-edge free shear layer is severed from the separation envelope. The remains of the layer attached to the leading edge continues to rollup at $\Delta t^* = 0.72$, inducing flow toward the airfoil surface. In this manner, the flow becomes reattached with the formation of a leading-edge vortex. The shear layer continues to feed the leading-edge vortex at $\Delta t^* = 1.5$. During this period the remnants of the baseline separation envelope are convected along the chord, replaced by the advancing leading-edge vortex which continues to appreciate in size and extend the region of reattachment. By $\Delta t^* = 2.42$ the recirculatory region extends the entire length of the airfoil and

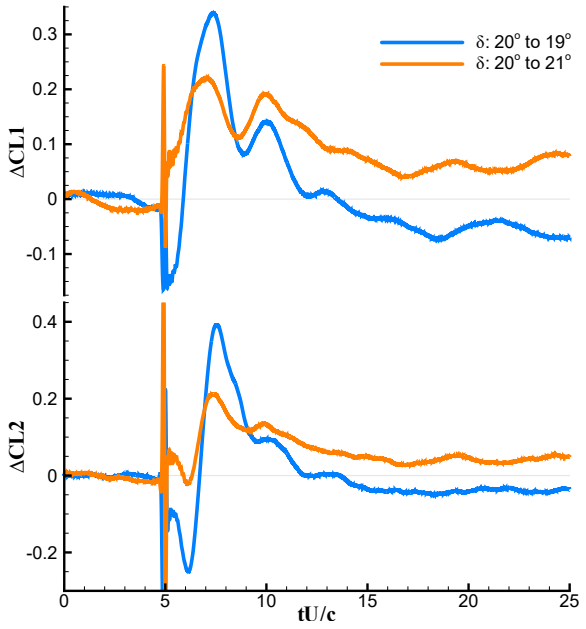

Figure 6: $\alpha_{\mathrm{LE}} = 20°$

coincides with peak lift production. Beyond this point the circulatory region is gradually removed from the airfoil surface, particularly the trailing-edge region, as the relaxation process converges to the massively separated state once again.

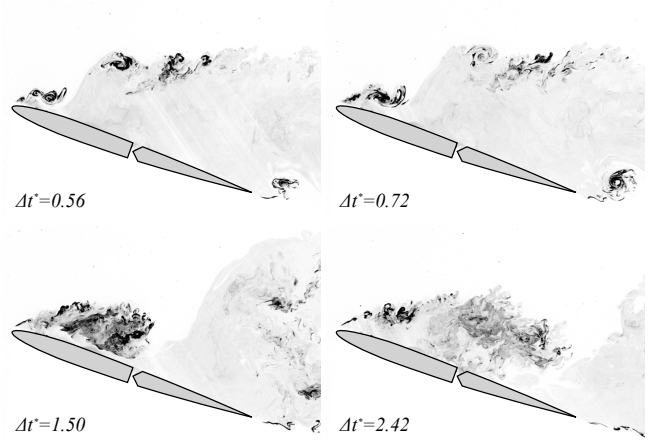

Figure 7: $\alpha_{\mathrm{LE}} = 20°$, $\delta = 20° \rightarrow 19°$, $6Hz$

Previously it was noted the transient lift profiles garnered in $\pm 1°$ step deflections differed primarily in temporal magnitude. As such, it would be rather plausible that the mechanisms by which the lift transients are produced in both step cases are quite similar and rudimental to massively separated flows. To this end, we note a comparable evolution of the flow for $\Delta\delta = +1°$ in Fig. 8. Shortly after the step at $\Delta t^* = 0.56$ there exists a distinct vortical formation within the shear layer near the leading edge. This formation, akin to that of the

previous case, effectively disrupts the shear layer from feeding the separation envelope. As a result, a leading-edge vortex is created and proceeds to entrain the surrounding flow field toward the airfoil surface. By $\Delta t^* = 1.5$ the entrainment process does not appear as effective as the previous case of negative-camber step but provides a similar byproduct of shedding the baseline separation envelope.

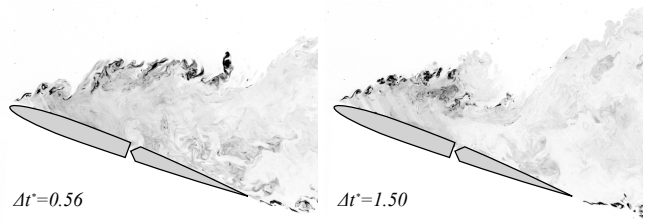

Figure 8: $\alpha_{\mathrm{LE}} = 20°, \delta = 20° \rightarrow 21°, 6Hz$

The receptivity of the representative massively separated flow has become apparent, showcasing rollup of the free shear layer culminating in the formation of a leading-edge vortex independent of step direction. Returning focus back to the separated case of $\alpha = 10°$ the response of the flow is mitigated to flow reattachment. Fig. 9 provides flow field snapshots for a negative-camber step input. Upon completing the flap motion, the shear layer is drawn to the airfoil and ceases to feed the separation envelope. As time progresses the packet of vorticity drawn from the shear layer convects downstream, adhering to the contour of the airfoil surface. That is, the step of the flap is sufficient to momentarily reattach the flow for several convective times. As shown in Fig. 9, at $\Delta t^* = 2.42$ the entirety of the airfoil is now reattached with a well-behaved trailing edge shear layer. Although the flow field is devoid of large scale leading-edge vortex formations, the process of reattachment introduces significant structures as the initial separation envelope is supplanted by the reattached boundary layer. Upon relaxation the flow is returned to its baseline separated state.

To similar effect, a positive-camber step also proves disruptive to communication between the free shear layer and the separation envelope, as shown in Fig. 10. The ensuing boundary layer, however, appears to host larger vortical elements conducive to elevated lift production. Through these investigations it appears excitation by a low-amplitude rapid ramp of the trailing-edge flap deflection is sufficient to garner an immediate aerodynamic response. Within the representative separated flow field, only the positive-camber step of $\Delta\delta = 1°$ produced a net increase in transient lift. The response of the representative massively separated flow provided a tradespace between accelerated (instantaneous) realization of long-time lift and peak lift production offered by a positive-camber and negative-camber step, respectively.

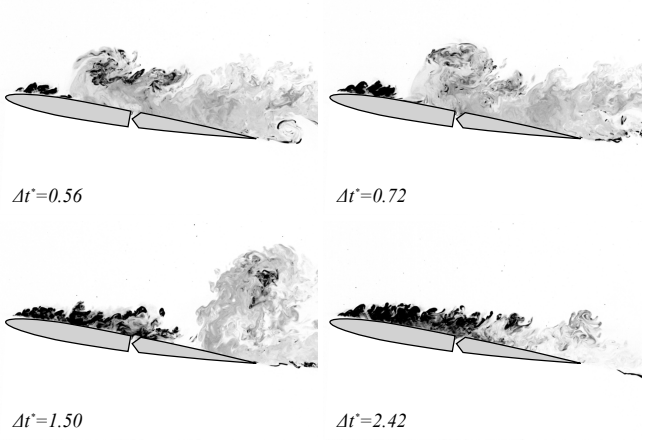

Figure 9: $\alpha_{\mathrm{LE}} = 10°, \delta = 10° \rightarrow 9°, 6Hz$

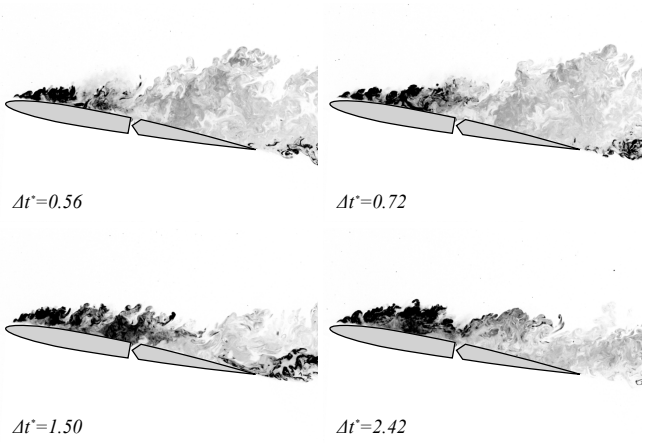

Figure 10: $\alpha_{\mathrm{LE}} = 10°, \delta = 10° \rightarrow 11°, 6Hz$

3.4 *Periodic Flap Actuation*

Conventional fluidic actuators have showcased the utility of continuous or periodic excitation to great effect on separated flows. These demonstrations often entail establishing and maintaining reattachment under sustained excitation for steady cruise conditions at elevated angles of attack. As we have employed mechanical actuation of the flap as a surrogate for bound circulation pulsing the prospect of periodic actuation presents a dilemma: due to geometric constraints the flap cannot provide continuous excitation of desired direction. If sequential pulses/steps of $\Delta\delta = -1°$ are desired, for example, the flap would require a return phase of motion as the flap is reset in preparation for the subsequent pulse. With this consideration, this study proceeds with focus given to the separated state of $\alpha_{\mathrm{LE}} = 10°$ subjected to a sinusoidal flap schedule given the insensitivity of the transient profile (Fig. 3) to step direction and the relative agreement of transient flow structures among both step cases (Fig. 9, 10). The sinusoidal deflection cycle is performed about a mean flap

angle of $\delta = 10°$ with a deflection amplitude of $\Delta\delta = 1°$, with a peak-to-peak sweep angle of $2°$ ($\delta = 11° \rightarrow 9°$). The frequency of flapping is derived from the desire to invoke a shedding event on the order of one convective time to affirm some measure of authority over the wake. This equates to a Strouhal number of $St = 0.175$ which is well within the reported bounds of shedding ($St = 0.13 - 0.20$) [9]. Such a display is made all the more remarkable considering the transitional state of the $\alpha = 10°$ near-body wake.

The phase-averaged lift history for a sinusoidal flap cycle is presented in Fig. 11. The phase-averaged lift curves were generated from a series of 100 flap cycles where the initial and final 10 cycles of measurement were discarded from the averaging scheme to remove starting transients and stopping effects. Among the actuation rates there is a general trend of increasing lift amplitude with increasing Strouhal number. Shortly after peak acceleration phases of motion ($t/T = 0.0$ and 0.5) trends show a global minimum and maximum. However, global lift peaks are not entirely in phase with acceleration and the overall lift profile exhibits quite a bit of undulation throughout the flap cycle indicating the forces generated are not superficially owed to dominance of non-circulatory added mass effects. Of these cases particular interest is given to the lift history of Strouhal number $St = 0.175$, corresponding to a frequency of $f = 1.0Hz$. That is, one flap cycle is completed over one convective time. Further, vortex shedding of the supercritical Hopf bifurcation regime is typically observed within $St = 0.13 - 0.2$. However, for $Re = 4 \times 10^4$ the near wake is understood to be in transition for an airfoil fixed at $\alpha = 10°$. The question remains as to whether the low-amplitude sinusoidal kinematics of the flap are sufficiently influential to impose some regularity or authority over the shedding pattern in the near-body wake to a representative case of $St = 0.175$.

A sense of repeatability of the lift cycle is provided by observation of Fig. 12 which presents the cycle-to-cycle variation of lift coefficient with deflection angle. Transient cycles (the first 10 cycles) are highlighted to differentiate from cycles included in the phase-averaging of Fig. 11. The black loops are considered fully-developed and relatively free of starting transients. Although transient cycles demonstrate a gradual drift toward the 'fully developed' periods there does not appear to be major transformations in hysteresis characteristics among the entirety of the run cycles. Indeed, once fully developed there does appear to be cycle-to-cycle variation in mean lift, however, importantly there does not appear to be discernible shift in phase between flap angle and lift history.

It is well understood that the near-body wake dynamics can bear a significant influence on aerodynamic loading. To examine the extent of lock-in, the near-body flow field of the wing is quantified by particle image velocimetry. The interrogation window is situated 2.5 chord downstream of the airfoil leading edge. A snapshot of the vorticity field is provided in the sub-diagram of Fig. 13. Initial inspection of vorticity shows a trail of vorticity packets convecting downstream. To quantify the the frequency content of this wake dynamic mode decomposition is performed, where the normalized mode amplitudes are presented in Fig. 13 along with the first four dynamic modes. Mode 1 reflects the signature of a mean vorticity field and is of the largest amplitude among the modes. Mode 2 is the second largest amplitude and corresponds to patterns congruent to the sizing of the vorticity concentrations. It is noted that the frequency associated with Mode 2 also matches the driving frequency of the sinusoidal flap maneuvers. This observation, coupled with the relatively abrupt decline of subsequent mode amplitudes, would indicate that by actuation of the trailing-edge flap some measure of authority may be retained, or rather reinstated, over the near-body shedding frequency even in a transitional operation space.

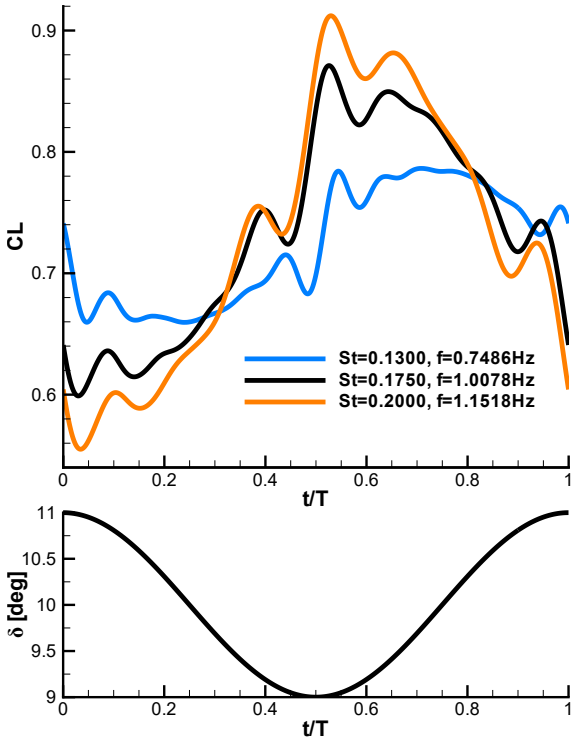

Figure 11: (*top*) Phase-averaged lift cycle variation with Strouhal number. (*bottom*) Flap deflection cycle.

4 Conclusion

The current effort to examine the response of a separated flow to rapid mechanical actuation of a trailing-edge flap included step-and-hold and continuous harmonic flapping maneuvers. In both kinematic maneuvers the amplitude of motion was limited to $1°$. In step-and-hold the flap was employed as a surrogate for a bound circulation impulse. It was found upon completing the maneuver the transient lift

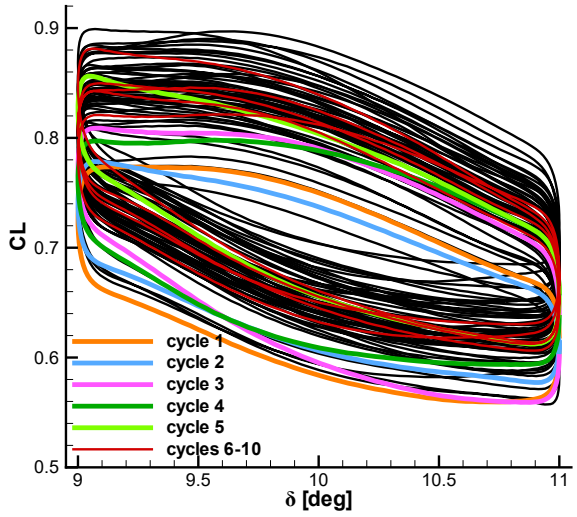

Figure 12: Lift hysteresis and cycle-to-cycle variation for $\alpha = 10^\circ$ under sinusoidal flapping.

profile would experience an instantaneous shift in magnitude dependent on the direction of step. The resulting lift history for the representative separated case of $\alpha = 10^\circ$ did not appear to display modification to the overall lift profile trends in response to flap step direction. However, for a massively-separated case of $\alpha = 20^\circ$ the transient lift profile experienced temporal modification to scaling. It was also noted that a positive-camber step in both separated and massively separated states amounted to an instantaneous attainment of the long-time steady lift value associated with the final hold geometry. This is interpreted as a potential avenue to expand the limited bandwidth of conventional control techniques in the perspective of feedback control. The temporal scaling of profile magnitude experienced for the massively separated case appeared to correlate with the effectiveness of the flap to induce rollup of the leading-edge shear layer. When the flap was engaged in continuous harmonic pitching at $\alpha = 10^\circ$ we were able to demonstrate authority over the near-body wake shedding behavior. The combination of attack angle and Reynolds number ensured the airfoil wake is in transition, external to the shedding guidelines of $St = 0.13 - 0.20$. However, quantification of the wake revealed the flap was sufficient to impose a shedding pattern corresponding to $St = 0.175$. Lock-in of the wake and large scale shedding was verified by application of dynamic mode decomposition.

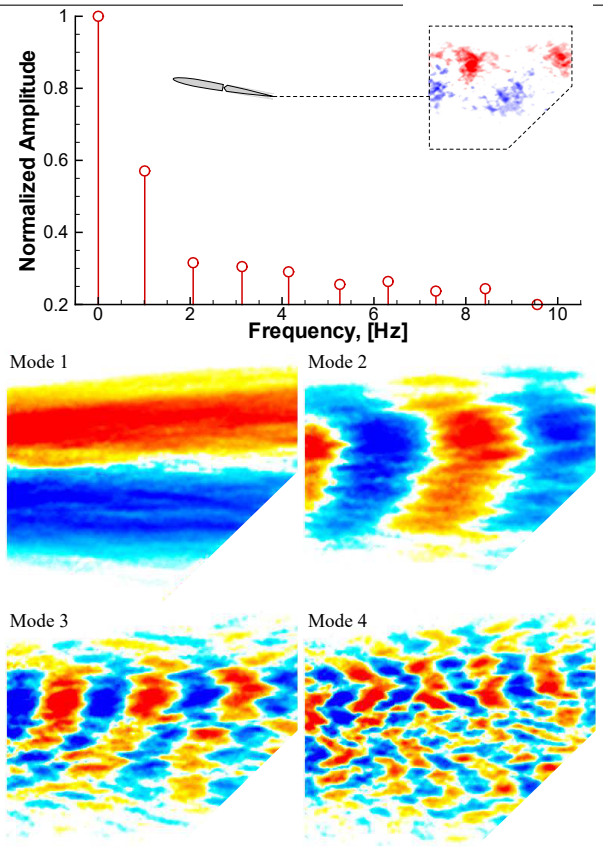

Figure 13: DMD of the near-body vorticity field: (*top*) normalized mode amplitude, (*bottom*) select modes.

References

[1] A. Seifert, T. Bachar, D. Koss, M. Shepshelovic, and I. Wygnanski. Oscillatory blowing: A tool to delay boundary layer separation. *AIAA Journal*, 31(11):2052–2060, 1993.

[2] A. Seifert, A. Darabi, and I. Wygnanski. Delay of airfoil stall by periodic excitation. *Journal of Aircraft*, 33(4):691–698, 1996.

[3] W. Kerstens, J. Pfeiffer, D. Williams, R. King, and T. Colonius. Closed-loop control of lift for longitudinal gust suppression at low reynolds numbers. *AIAA Journal*, 49(8):1721–1728, 2011.

[4] W. McCroskey. Unsteady airfoils. *Annual Review of Fluid Mechanics*, 14(1):285–311, 1982.

[5] K.R. Sreenivasan, P.J. Strykowoski, and D. J. Olinger. Hopf bifurcation, landau equation, and vortex shedding behind circular cylinders. In *Forum on Unsteady Flow Separation*, volume 52, pages 1–13, 1987.

[6] J. Choi, T. Colonius, and D.R. Williams. Surging and plunging oscillations of an airfoil at low reynolds number. *J. Fluid Mech.*, 763:237–253, 2015.

[7] S.T.M. Dawson, D.C. Floryan, C.W. Rowley, and M.S. Hemati. Lift enhancement of high angle of attack airfoils using periodic pitching. In *2016 AIAA Aerospace Sciences Meeting, AIAA SciTech Forum*, 2016.

[8] D.J. Cleaver, Z. Wang, and I. Gursul. Investigation of high-lift mechanisms for a flat-plate airfoil undergoing small-amplitude plunging oscillations. *AIAA Journal*, 51(4):968–980, 2013.

[9] R.F. Huang and C.L. Lin. Vortex shedding and shear-layer instability of wing at low-reynolds numbers. *AIAA Journal*, 33(8):1398–1403, 1995.

[10] H. Wagner. über die entstehung des dynamischen auftriebes von tragflügeln. *Zeitschrift für Angewandte Mathematic und Mechanik*, 5(1):17–35, 1925.

[11] A. Medina, M.V. Ol, P. Mancini, and A. Jones. Revisiting conventional flaps at high deflection rate. *AIAA Journal*, 55(8):2676–2685, 2017.

[12] A. Medina and M. Hemati. Separated flow response to rapid flap deflection. In *2018 AIAA Aerospace Sciences Meeting, AIAA SciTech Forum*, 2018.

[13] A. Medina, M.V. Ol, D.R. Williams, X. An, and M. Hemati. Modeling of conventional flaps at high deflection-rate. In *2017 AIAA Aerospace Sciences Meeting, AIAA SciTech Forum*, 2017.

[14] M .Ol, J. Eldredge, and C. Wang. High-amplitude pitch of a flat plate: an abstraction of perching and flapping. *International Journal of MAVs*, 1(3):203–216, 2009.